



## Original Article

## Effect of silk fibroin scaffold loaded with 17-β estradiol on the proliferation and differentiation of BMSCs



Juan Bai<sup>a, b, 1</sup>, Haotian Li<sup>c, 1</sup>, Lu Wang<sup>a, b, 1</sup>, Yue Shi<sup>b</sup>, Xiaomin Su<sup>b</sup>, Changzhen Xu<sup>b</sup>, Qiaoling Guo<sup>b</sup>, Jing Feng<sup>b</sup>, Xilin Sun<sup>b</sup>, Yitong Cheng<sup>b</sup>, Jie Kang<sup>b</sup>, Jiayu Wen<sup>b</sup>, Feng Wu<sup>b, \*</sup>

<sup>a</sup> Department of Prosthodontics, Shanxi Medical University School and Hospital of Stomatology, Taiyuan, 030001, China

<sup>b</sup> Shanxi Province Key Laboratory of Oral Diseases Prevention and New Materials, Taiyuan, 030001, China

<sup>c</sup> First Clinical Medical College of Shanxi Medical University, Taiyuan, 030001, China

## ARTICLE INFO

## Article history:

Received 20 November 2022

Received in revised form

16 February 2023

Accepted 9 March 2023

## Keywords:

Silk fibroin

17-β estradiol

Silk fibroin porous scaffolds

BMSCs

## ABSTRACT

In this study, different concentrations of 17-β estradiol silk fibroin (SF)porous scaffolds (SFPS) were prepared using freeze-drying technique, with a hope for optimal concentration and apply it locally to the bone defect area. In this study, the porous scaffold morphology structure was characterized by SEM, FTIR and universal capacity testing machines, and the in vitro cytocompatibility and biological activity of scaffold materials were studied by cell adhesion, viability and proliferation experiments. The results showed that SFPS boasts better physicochemical properties, while 17-β estradiol SF scaffolds with low concentrations of 10<sup>-10</sup> mol/L and 10<sup>-12</sup> mol/L had more growth and proliferation of SF scaffolds with higher concentrations, and 10<sup>-10</sup> mol/L was the optimal concentration of 17-β estradiol SFPS, which was more conducive to cell adhesion and proliferation. On the other hand, after osteogenesis induction of BMSCs inoculated on 17-β estradiol SFPS at different concentrations, it was found that the expression of alkaline phosphatase in BMSCs on different concentrations of 17-β estradiol porous scaffolds was not large. No conflict of interest exists in the submission of this manuscript.

© 2023, The Japanese Society for Regenerative Medicine. Production and hosting by Elsevier B.V. This is an open access article under the CC BY-NC-ND license (<http://creativecommons.org/licenses/by-nc-nd/4.0/>).

## 1. Introduction

Oral and maxillofacial bone defects caused by accidents (traffic, labor, sports, shooting), surgical removal of benign lesions (cysts, dental tumors) or malignant tumors, congenital deformities such as fissures, visceral skull dysplasia, periodontitis, dental abscesses or tooth extraction will not only cause functional disorders such as chewing, swallowing, and sucking, but also destroy the facial shape, reducing the aesthetics of the oral and maxillofacial area [1]. With the development of bone reconstruction, many approaches are available to repair these jaw defect areas, such as bulk autologous bone grafting technique (Onlay technique) [2], stretch osteogenesis [3], bone tissue engineering [4]. Among them, the second is

considered the “gold standard”. Yet, it's come with limited sources, complications and other defects [5]. Stretch osteogenesis makes more bone mass possible, but it's accompanied by excessive trauma and requirement of early-stage hospitalization. Bone tissue engineering offers a new solution, which has received extensive attention and becomes a research hotspot.

Estrogen is subjected to C-18 steroid characterized by the presence of an aromatic ring on C-3. There is a phenolic hydroxyl group on C-3 and a hydroxyl group (estradiol) or one ketone (estrone) on C-17. During their lifetime, women produce three types of estrogens, including 17-β estradiol (17-β estradiol E2) from puberty to menopause, estriol E3 during pregnancy, and estrone (Estrone E1) after menopause [6], of which 17-β estradiol is the most abundant and important one. Estrogen is essential for bone growth and development and for maintaining bone health in adulthood [7,8]. Since estrogen is important for bone balance regulation, its deficiency represents one of the primary causes of osteoporosis in postmenopausal women [9], causing changes in the balance, bone structure, and bone resorption activity of the cells that make up the bone marrow.

\* Corresponding author. School and Hospital of Stomatology, Shanxi Medical University, Taiyuan, 030001, China

E-mail address: [wfmjh@163.com](mailto:wfmjh@163.com) (F. Wu).

Peer review under responsibility of the Japanese Society for Regenerative Medicine.

<sup>1</sup> These authors contributed equally to this paper.

It has been shown that estrogen can regulate a variety of bone metabolism factors, which could directly or indirectly be involved in the regulation of bone marrow mesenchymal stem cells and osteoblastic progenitor cell differentiation. Also, estrogen could promote the synthesis and secretion of osteoprotectin (OPG), inhibit the secretion of interleukin 1 (IL-1), interleukin 6 (IL-6), tumor necrosis factor  $\alpha$  (TNF- $\alpha$ ), prostaglandin (PGE2) and other bone resorption-related cytokines, thereby promoting osteogenesis and inhibiting bone breaking [10–12].

Bone Marrow Mesenchymal Stem Cells (BMSCs) offer multidirectional differentiation potential, allowing for differentiation of BMSCs into osteoblasts [13]. Besides, BMSCs could differentiate into multiple types of tissue cells with weak cell immunogenicity, vulnerable transfection of foreign genes, making it a hot spot in tissue engineering research and enjoying great prospects in gene and cell therapy.

Silk fibroin (SF) is a natural polymer organic material from silk with excellent properties [14,15]. Numerous studies have shown that SF represents an excellent biological material with good cellular compatibility and histocompatibility [16]. With an in-depth understanding of its intrinsic properties, such as mechanical strength, elasticity, biocompatibility and controllable biodegradability, SF has been made into films, porous scaffolds, hydrogels or non-woven nets [17–20], and are widely used in the repair and regeneration of skin, bone, blood vessels, nerves and other tissues.

Based on the above theories and previous studies, this study aimed for the effects of 17- $\beta$  estradiol silk fibroin porous scaffolds (SFPS) loaded with different concentrations on the proliferation and osteogenic differentiation of BMSCs. SFPS loaded with 17- $\beta$  estradiol were prepared by freeze-drying and the physicochemical properties of the scaffolds were characterized. Afterwards, BMSCs were seeded on SFPS loaded with different concentrations of 17- $\beta$  estradiol, and the effects of different concentrations of 17- $\beta$  estradiol on the proliferation and differentiation of BMSCs were observed, hoping to find the optimal concentration and apply it locally to the bone defect area. As such, it could clinically repair the oral and maxillofacial bone defect area, shortening the healing time of bone augmentation surgery, and providing a new idea for new therapies for bone defect.

## 2. Materials and methods

### 2.1. Materials

*Bombyx mori* raw silk fibers were purchased from Dingsheng Silk Co. Ltd (Wujiang, China); Bone Marrow Mesenchymal Stem Cells were purchased from Tongpai Biotech-nology Co. Ltd. (Shanghai, China); Dulbecco's Modified Eagle's Medium (DMEM) and fetal bovine serum (FBS) were purchased from Gibco Invitrogen; Dexamethasone, L-ascorbic acid and b-glycerophosphate were purchased from Cyagen Biological Tech Co. Ltd. (Guangzhou, China); The cell counting kit-8 (CCK-8) was purchased from Boster Biological Tech Co. Ltd. (Wuhan, China); The living/dead cell staining kit (Calcein-AM/PI double staining method) was supplied by BestBio Biological Tech Co. Ltd. (Shanghai, China); The reagents used in this study were of analytical grade and used without any further purification. The deionized ultra-pure water was used throughout the experimental trials.

### 2.2. Preparation of SF solution

SF solution was prepared based on the methods mentioned in the published papers [21–24]. That is to say, household silk is degummed in Na<sub>2</sub>CO<sub>3</sub> (0.05wt%) solution at 100 °C for 30 min, repeatedly treated three times, rinsed thoroughly with distilled

water, and dried overnight in a drying box at 60 °C. The degummed silk fibers were dissolved with CaCl<sub>2</sub>: CH<sub>3</sub>CH<sub>2</sub>OH: H<sub>2</sub>O (molar ratio of 1:2:8) ternary solution at 72 °C for 40min. Use a dialysis bag with an intercepted molecular weight of 8000–14000 to remove the inorganic salts by dialysis for 4 d at room temperature, then centrifuge at 3000 r/min for 5min, and store the clear in a refrigerator at 4 °C.

### 2.3. Preparation of 17- $\beta$ estradiol silk fibroin solution at different concentrations

Weigh 27.238 mg of 17- $\beta$  estradiol powder, dissolve it in 10 ml of absolute ethanol with an ultrasonic cleaning machine, and prepare 10<sup>-2</sup> mol/L of 17- $\beta$  estradiol stock solution 1; Take 100  $\mu$ l of 17- $\beta$  estradiol stock solution 1 dissolved in 10 ml of phosphate buffered saline PBS to obtain 10<sup>-4</sup> mol/L of 17- $\beta$  estradiol stock solution 2. PBS stock solution 2, 3, 4 and 5 containing 10<sup>-4</sup> mol/L, 10<sup>-6</sup> mol/L, 10<sup>-8</sup> mol/L, and 10<sup>-10</sup> mol/L of 17- $\beta$  estradiol was finally obtained by gradient dilution. Add 30% glycerol to 10 ml of 4wt% SF solution to obtain a SF solution that does not contain 17- $\beta$  estradiol; Similarly, a 17- $\beta$  estradiol silk protein solution containing 0, 10<sup>-6</sup> mol/L, 10<sup>-8</sup> mol/L, 10<sup>-10</sup> mol/L 10<sup>-12</sup> mol/L was obtained by gradient dilution.

### 2.4. Preparation of 17- $\beta$ estradiol SFPS

In this experiment, different concentrations of 17- $\beta$  estradiol silk protein solution prepared according to the above method were injected into a silica gel tube with a diameter of 8 mm and a height of 2 cm, the bottom of the silicone tube was close to the -80 °C subcooling surface, the top was open, frozen in a -80 °C low-temperature freezer for 24 h, vacuum freeze-dried for 36–48 h, and a 17- $\beta$  estradiol SFPS was obtained.

### 2.5. Performance characterization of materials (scanning electron microscopy, infrared spectroscopy)

The above five groups of material samples were vacuumed, and sprayed with gold, and their morphology was observed by JSM-7001 F scanning electron microscope (SEM). Image J software was used to measure and analyze the aperture size of the porous scaffold.

The Fourier transform infrared (FTIR, Bruker, Germany) spectroscopy was used to measure the absorption spectra of the above five groups of porous scaffold materials with a wavelength of 4000–400 cm<sup>-1</sup> and perform infrared spectral analysis.

### 2.6. Degradation study

The freeze-dried composite scaffolds material (n = 3) was weighed and placed in a 24-well plate and incubated at 37 °C in PBS buffer containing 1U/mL proteinase-XIV for 14 d. Fresh PBS buffers (with and without enzymes) should be replaced every 3 d. At the specified time point, the relevant sample is removed and carefully and thoroughly washed with deionized water to ensure that the material does not contain enzymes. After freeze-drying, the mass loss percentage was weighed and analyzed [24].

### 2.7. Analysis of mechanical properties of materials

Different concentrations of 17- $\beta$  estradiol SF solution were made into a cylindrical shape with a diameter of 26 mm and a height of 12 mm, and the mechanical properties of the porous scaffold were determined by a universal ability testing machine. In the experiment, a 1000 N sensor was used to compress the material thickness

to 9 mm ( $n = 5$ ) at a speed of 0.2 mm/min, and the elastic modulus ( $E$ ) and compressive strength ( $P$ ) of the porous scaffold were determined according to the following formula.

$$P = \frac{F}{S} \quad (F : \text{force}, S : \text{area of square})$$

$$E = \frac{P}{\Delta L/L} \quad (P : \text{pressure}, \Delta L : \text{change in length}, L : \text{length})$$

## 2.8. E2 release from SFPS

The 17- $\beta$  estradiol SFPS ( $8 \times 10$  mm) were immersed in 4 ml of PBS solution and incubated at 37 °C with gentle shaking (50 rpm). At specific time points, the 3 ml PBS solution was collected and used for the estimation of released E2 using ELISA assay (17- $\beta$  E2 ELISA kit, Shanghai Hengyuan Biological). The scaffolds were then replenished with 3 ml of fresh PBS. This process was repeated until the completion of the study.

## 2.9. Cell compatibility and osteogenic activity studies

### 2.9.1. Cell proliferation and adhesion experiments

Cut the  $8 \times 10$  mm SF scaffold into 1 mm thick slices and sterilize using autoclaving.  $3 \times 10^5$ /well BMSCs were seeded on five 17- $\beta$  estradiol scaffolds of different concentrations, 5 control groups were set up for each sample, and when BMSCs were cultured on scaffold material for 1 d, 4 d, 7 d, and 10 d, respectively, the scaffold was placed on a new plate and 500  $\mu$ l of DMEM (Dulbecco S Modified Eagle Medium) medium and 50  $\mu$ l of CCK-8 (Cell Counting Kit-8) working solution, and at the same time, 500  $\mu$ l of DMEM and 50  $\mu$ l of CCK-8 working solution were added to the scaffold material as a blank control. Incubate in a 37 °C, 5% CO<sub>2</sub> incubator for 1 h, then transfer 100  $\mu$ l of each well to a 96-well plate, and the microplate reader determines the Optical density OD value at a wavelength of 450 nm and calculates its survival rate.

Fluorescent staining observed the surface adhesion of bone marrow mesenchymal stem cells to determine their proliferation. The cells were seeded on each set of scaffolds, cultured for 1 day, 4 days, and 7 days, then the original culture medium was aspirated and discarded. Subsequently, 1 ml of paraformaldehyde fixative solution (2.5%) was added per well, followed by 0.5% TritonX-100 solution for penetration. Then add 500-fold diluted rhodamine-phalloidin staining solution under dark conditions for staining. Add DAPI staining solution for nuclear staining. Finally, the state of the cytoskeleton and nucleus is observed under a laser scanning confocal microscope (LSCM).

Cells were seeded on each set of scaffolds at a density of  $1 \times 10^4$  cells/well and cultured for 7 days. Discard the medium and wash the PBS solution. Then, an appropriate amount of 4% paraformaldehyde is added within each well and the cells are fixed at 4 °C for 4 h. After washing the PBS solution, dehydrate with 20%, 40%, 60%, 80%, and 100% gradient alcohol. Finally, the cells are naturally dried and subjected to scanning electron microscopy after gold spraying.

### 2.9.2. Live/dead cell staining experiments

To detect the viability of cells on scaffolds, cells are seeded on each set of scaffolds. After incubating at 37 °C, 5% CO<sub>2</sub> for 1 d, 4 d, and 7 d, remove the stent from the well plate and wash 3 times with sterile PBS. Then, follow the manufacturer's (live/dead cell staining kit) to stain for calcein (AM) and propidium iodide (PI). Place the stained scaffold at room temperature or 37 °C for the reaction for 30 min. After washing with PBS, observe the growth of cells on the

scaffold using LSCM at a wavelength of 488 nm. Live cells and scaffold-attached cells appear green (green calcein: Ex/Em 490/515 nm; Red PI: Ex/Em 535/617 nm).

### 2.9.3. ALP detection

BMSCs were induced to osteogenesis with a medium supplemented with 10 mM  $\beta$ -glycerophosphate sodium (Sigma-Aldrich), 10 nM dexamethasone (Sigma-Aldrich) and 50  $\mu$ g/ml antioxidant acid (Sigma-Aldrich), induced 4 d, 7 d, 14 days and tested with ALP kit, and 4 samples per group were washed with 4% paraformaldehyde. Qualitative staining was performed with an ALP staining solution. Subsequently, the specimen is rinsed with PBS and lysed with 2% Triton X-100. Select the 96-well plate and measure the OD at 510 nm as described in the Alkaline phosphatase ALP kit (Leagene, Beijing).

## 2.10. Statistical analysis

In this study, data were expressed as mean  $\pm$  standard deviation or median and quartiles, as appropriate. The test level is set at  $\alpha = 0.05$ , and  $P < 0.05$  indicates a significant difference. SPSS (26.0) and R (3.2.0) were used for data analysis. LSD-t test and Scheirer-Ray-Hare rank sum test were used for difference comparison, as appropriate.

## 3. Results

### 3.1. Microscopic morphology of SFPS

As shown in Fig. 1, the SFPS features a uniform porous structure, in which the pore structure is interconnected. With the increase of estradiol concentration of 17- $\beta$ , the pore structure of the SF porous scaffold didn't show a sign of significant change, with the pore size of the measured multi-porous scaffold reaching an average of  $113.85 \pm 3.3$   $\mu$ m.

### 3.2. Secondary structure analysis of porous scaffolds

The molecular conformation of the 17- $\beta$  estradiol SFPS was characterized by infrared spectroscopy. According to previous studies on infrared absorption spectroscopy of SF materials, the absorption peaks of Silk I appeared near 1650–1655  $\text{cm}^{-1}$  (amide I), 1525–1540  $\text{cm}^{-1}$  (amide II), 1266  $\text{cm}^{-1}$  (amide III) and 669  $\text{cm}^{-1}$  (amide V). The absorption peaks of Silk II occurred around 1620–1635  $\text{cm}^{-1}$  (amide I), 1515–1530  $\text{cm}^{-1}$  (amide II), 1230–1235  $\text{cm}^{-1}$  (amide III), and 700  $\text{cm}^{-1}$  (amide V). Also, random coiled absorption peaks occur around 1655–1660  $\text{cm}^{-1}$  (amide I), 1535–1545  $\text{cm}^{-1}$  (amide II), 1235  $\text{cm}^{-1}$  (amide III), and 650  $\text{cm}^{-1}$  (amide V) [24]. As shown in Fig. 2, the five groups of curved absorption peaks appeared at 1232  $\text{cm}^{-1}$ , 1517  $\text{cm}^{-1}$ , and 1623  $\text{cm}^{-1}$ , showing a typical Silk II, while the molecular structure was not significantly different between the different groups.

### 3.3. Analysis of mechanical properties of materials

Mechanical properties are one of the important technical parameters for the study of various biological materials. Those biomaterials for tissue engineering scaffolds must have a certain mechanical strength for the effective promotion of the repair and regeneration of supporting tissues. Fig. 3 demonstrates the stress-strain curve of the SFPS. The compressive strength and elastic modulus of the stent material were  $26.37 \pm 4.25$  kPa,  $83.86 \pm 9.77$  kPa, respectively.

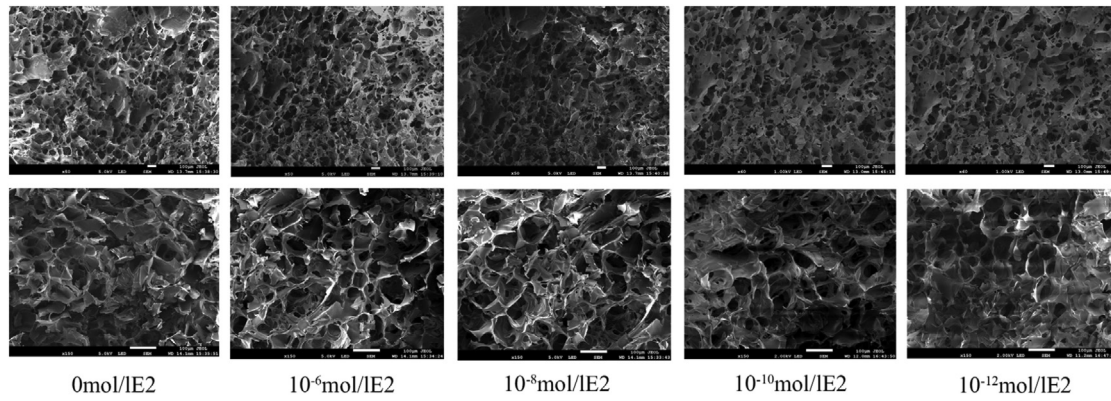


Fig. 1. 17-β estradiol SFPS SEM at different concentrations.

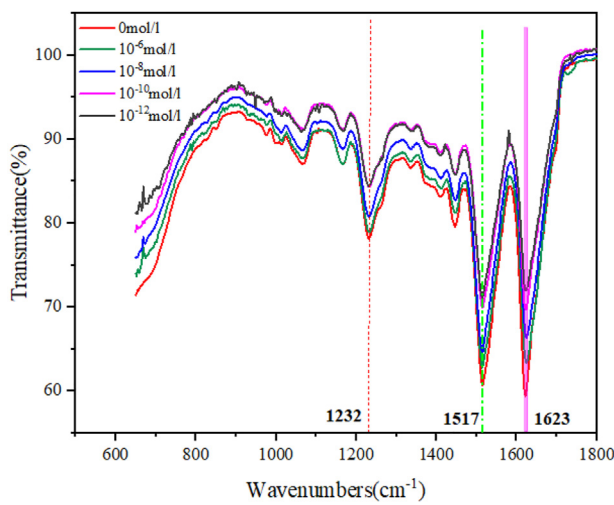


Fig. 2. FTIR spectra of SFPS with different concentrations of 17-β-estradiol.

3.4. Degradation behavior

Fig. 4 shows the quality change of silk fibroin porous scaffolds during degradation. It can be seen from the figure that the mass loss

of the scaffold increases with the extension of degradation time. When the scaffold is immersed in enzyme solution for 14 days, the mass loss reaches 50.31%.

3.5. The release of E2 from SFPS

As shown in Fig. 5, sudden release of silk fibroin scaffolds of different concentrations occurred 4 days before the release. With the extension of time, the drug release rate slowed down, but the slow release effect was not obvious. On the 10th day of drug release, the drug release amount reached about 50%.

3.6. Cell proliferation and adhesion experiments

The CCK-8 assay was used to study the viability and proliferation of cells in different concentrations of SF scaffolds. The results of CCK-8 cell proliferation assays (Fig. 6) showed that the cell proliferation rate was greater than 1 in all groups, and the cell proliferation rate was highest on day 7, followed by a decrease in cell proliferation rate. There was no statistical difference between the groups of cell proliferation on the scaffold materials of day 1 and day 4. Besides, by the 7th day, the number of cells on the five groups of scaffold materials was greatly proliferated, among which, the cells on the 17-β estradiol silk protein scaffold with different

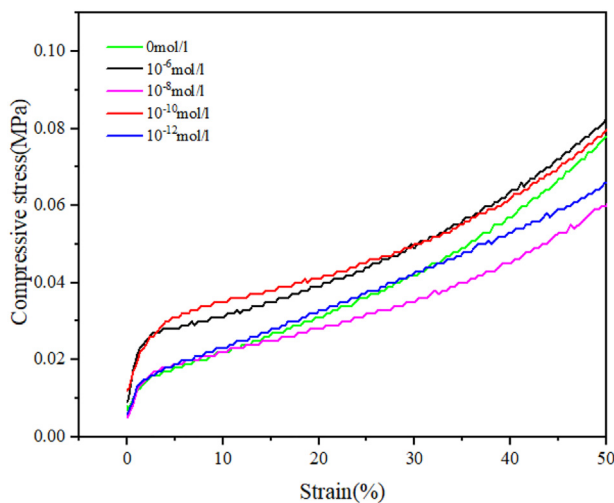


Fig. 3. Stress-strain curves of 17-β estradiol concentration SFPS at different concentrations.

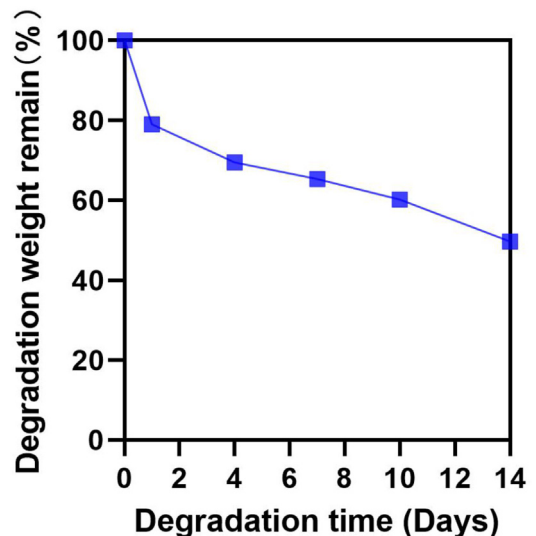


Fig. 4. Degradation curves of SFPS.

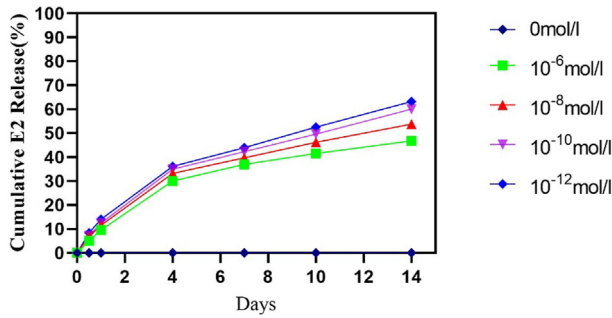


Fig. 5. Cumulative release profile of E2 from SFPS.

concentrations were more proliferating than the cells on the blank scaffold, with a significant statistical difference between the groups ( $P < 0.001$ ). Among them, the  $10^{-10}$  mol/L and  $10^{-12}$  mol/L 17-β estradiol silk protein scaffold cells with higher concentrations were proliferated, and the cells on the scaffold material of each group continued to proliferate after 10 days, with the same trend as the 7th day, and there were obvious statistical differences between the groups ( $P < 0.001$ ).

For cell adhesion, rhodamine-labeled phalloidin and DAPI were used to bind to F-actin and nucleus, respectively, and were analyzed using laser confocal microscopy. As shown in Fig. 7, there are a large number of cells attached to the inside of the SFPS, and the cells stretch and form a spindle-shaped. Also, rich stress fibers are formed by F-actin, and the cells proliferate rapidly, leading to a network-like fully mature cytoskeletal distribution, and tight junctions with surrounding cells. As time increases, BMSCs proliferated rapidly, and there were more obvious cell proliferations on the 17-β estradiol SF scaffold at different concentrations compared with the cells on the blank scaffold, among which the number of cells on the 17-β estradiol silk scaffold at  $10^{-10}$  mol/L and  $10^{-12}$  mol/L increased significantly.

SEM observations were consistent with laser confocal outcomes, and BMSCs showed good performance on all porous scaffolds. As shown in Fig. 8, after 7 days of in vitro culture, cells are tightly attached to the well wall, gathered into sheets, and wrapped in secreted matrix.

3.7. Live/dead cell staining experiments

We observed and tracked the viability of BMSCs inoculated on 17-β estradiol SFPS. As shown in Fig. 9, the results of calcein-am/PI dual staining showed that most BMSCs are bright green with a small number of dead cells (red fluorescence). As the culture time increases, the number of cells gradually increases. Additionally, compared with other concentrations of SF scaffolds, the number of cells of  $10^{-10}$  mol/L and  $10^{-12}$  mol/L 17-β estradiol silk protein

scaffolds with higher concentrations of SF scaffolds was significantly increased.

3.8. In vitro osteogenic induction differentiation of porous scaffold materials

The ALP activity of BMSCs cultured on SFPS for 4 days, 7 days, and 14 days is shown in Fig. 10. Different from cell proliferation experiments, ALP activity increased significantly at day 7 and decreased after day 14. The expression of BMSCs on 17-β estradiol SF scaffolds at different concentrations was consistent with that of alkaline phosphatase on BMSCs on blank scaffolds, not affecting the osteogenic differentiation of BMSCs.

4. Discussion

Estrogen plays an important role in the regulation of bone mass balance. Estrogen deficiency is one of the major reasons for osteoporosis in postmenopausal women. The lack of estrogen significantly changes the balance, bone structure, and resorptive activity of the cells that comprise the bone marrow [25,26]. Recently, it has been shown that 17-β estradiol (E2) can effectively enhance the proliferation and differentiation potential of BMSCs [27], but its effect on BMSCs concentration is disputed [28–31].

In this study, SFPS were used as the carrier to load different concentrations of 17-β estradiol on the scaffold, and the surface morphology, secondary structure and mechanical properties of the materials were first studied by SEM, FTIR and universal capacity testing machines. Through SEM observation, SFPS have relatively uniform pores, and the pore size is  $89.5 \pm 1.3 \mu\text{m}$  on average, which is within the optimal spatial range for cell growth [18]. Structural analysis by FTIR showed that SFPS were relatively subjected to stable Silk II structures. Mechanical properties are one of the important parameters of biological materials, any kind of biological materials should allow for sufficient mechanical properties to maintain the regeneration of new tissues Mechanical analysis shows that as scaffold material, SF scaffold offers a good modulus of elasticity, providing a more suitable biological environment for the growth of bone cells. The degradation rate of ideal scaffold material should match the growth rate of damaged tissue. The results of degradation experiments showed that with the progress of tissue repair, the scaffold material gradually degraded to provide space for new tissue. The drug release results show that the drug release effect of the stent is not obvious, and it can be further improved later.

Good cellular compatibility of scaffold materials is critical for tissue engineering [19]. Cell-scaffold materials require good connectivity and suitable pore size to enable cell migration and substance metabolism, as well as to support and induce tissue regeneration. To further analyze the biocompatibility of 17-β

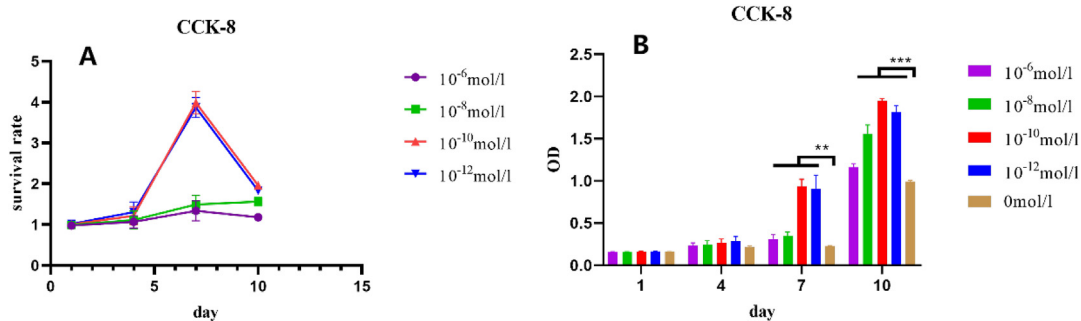
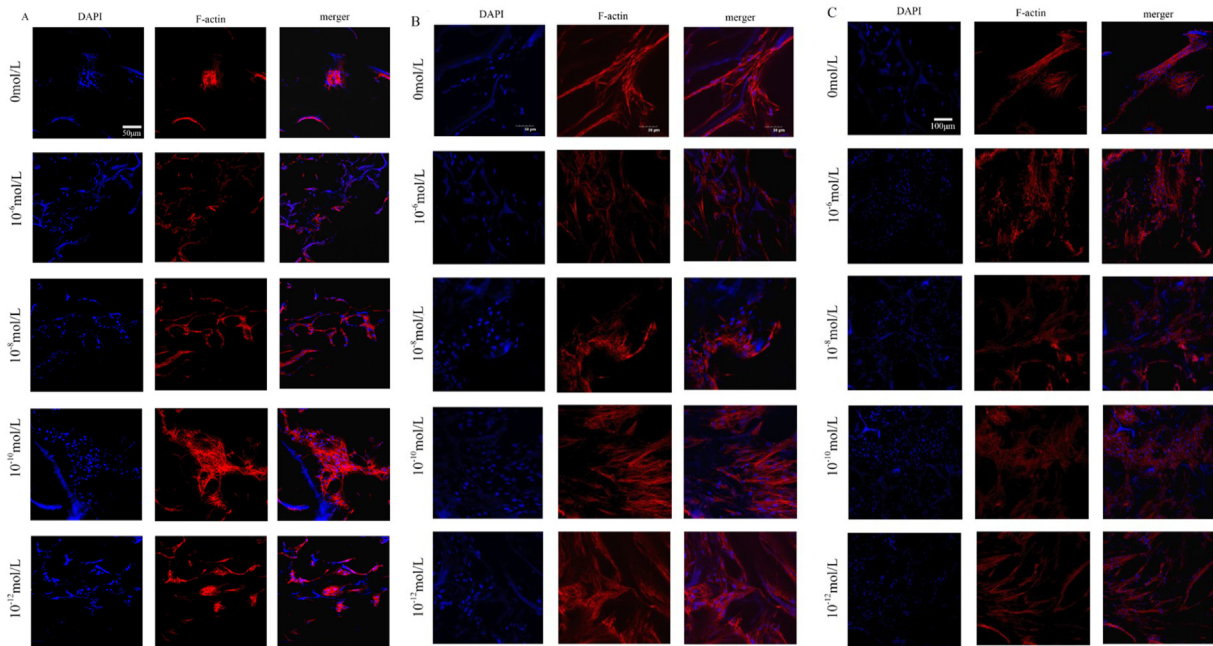
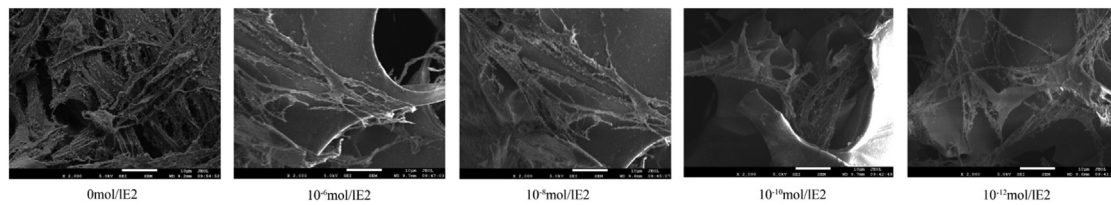


Fig. 6. Determination of survival (A) and absorbance (B) of 450 nm in different groups on day 1, 4, 7, and day 10 (\*\* $P < 0.01$ , \*\*\* $P < 0.001$ ).



**Fig. 7.** On the first day (A), the fourth day (B) and the seventh day (C) 17- $\beta$  The BMSCs cultured on porous scaffold with estradiol concentration silk fibroin were stained with Phalloidin DAPI. Blue stains for nucleus, red stains for cytoskeleton.



**Fig. 8.** Morphological observation of BMSCs on 17- $\beta$  estradiol SFPS at different concentrations.

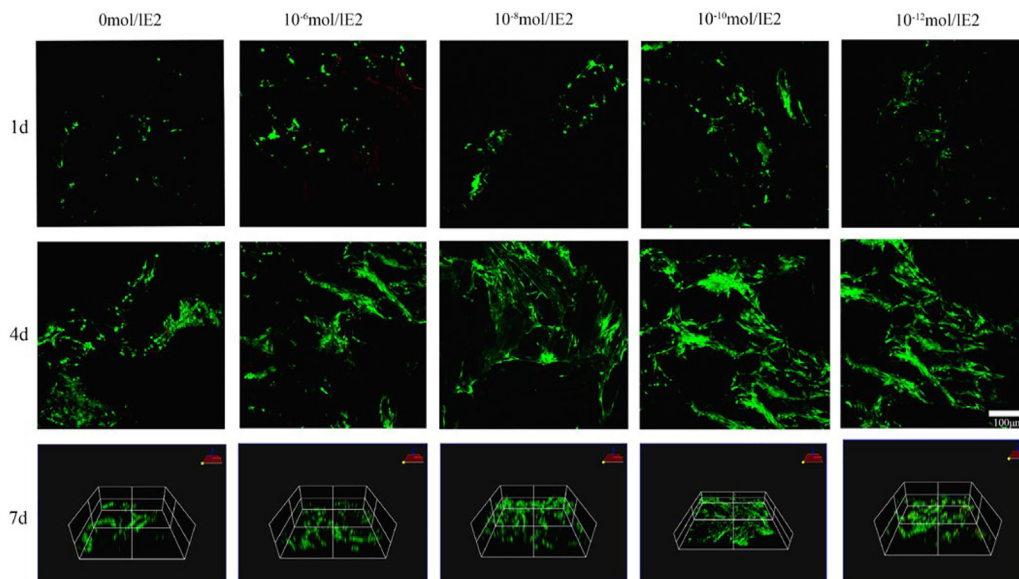


**Fig. 9.** Laser confocal microscopic images (2D) of BMSCs incubated on 17- $\beta$  estradiol concentration SFPS for 1 and 4 days. Laser confocal microscope images (3D) of BMSCs cultured for 7 days. Live cells are labeled with calcein (green) and dead cells with propidium iodide (red).

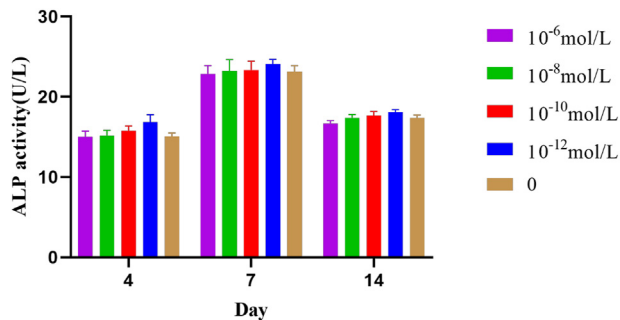


Fig. 10. ALP activity after 4 days, 7 days and 14 days of osteogenesis induction.

estradiol SFPS, BMSCs were seeded on 17- $\beta$  estradiol porous scaffolds at different concentrations, and LSCM was used to characterize cell viability in the cell-scaffold complex. After a total of 1 d, 4 d, 7 d, and 10 d, CCK-8 assay was used to quantitatively detect cell viability and proliferation on different scaffolds. SEM was used to observe the adhesion and morphological distribution of cells on the surface and inside each group of scaffolds. Based on the staining of live cells (green marker) and dead cells (red marker), the growth of cells on the scaffold was observed.

Overall, SEM images, LSCM images and CCK-8 analysis showed that SFPS had good biocompatibility, and BMSCs had a good growth trend in 17- $\beta$  estradiol silk protein scaffolds loaded with different concentrations, while cells with low concentrations of  $10^{-10}$  mol/L and 17- $\beta$  estradiol SFPS with higher concentrations of  $10^{-10}$  mol/L and  $10^{-12}$  mol/L had more growth and proliferation.  $10^{-10}$  mol/L is the optimal concentration of 17- $\beta$  estradiol SF porous scaffold, which is more conducive to cell adhesion and proliferation.

Of these, bone marrow mesenchymal stem cells (BMSCs) have the potential to differentiate into various types of cells, including osteoblast, and are found in various tissues including bone marrow, adipose tissue, umbilical cord blood, and cancellous bone [32]. Because of its high proliferation capacity, it is possible to directly perform cell transplantation or implantation on biological material to repair the defect of tissue. The activity of ALP is regarded as one of the characteristic parameters of osteoblast maturation, and its activity can reflect the tendency of differentiation to osteoblast.

ALP represents an early marker of osteogenic differentiation of BMSCs. In this study, we inoculated BMSCs on scaffolds, induced osteogenic differentiation, and measured ALP values. The results showed that the expression of BMSCs on 17- $\beta$  estradiol SF scaffolds at different concentrations was consistent with the expression of alkaline phosphatase on BMSCs on blank scaffolds, and different concentrations of 17- $\beta$  estradiol had no effect on osteogenic differentiation of BMSCs.

## 5. Conclusion

In this study, different concentrations of 17- $\beta$  estradiol silk fibroin (SF) porous scaffolds (SFPS) were prepared using freeze-drying technique. Through experiments, we found that  $10^{-10}$  mol/L represents an appropriate concentration of 17- $\beta$  estradiol SFPS, which could be applied to bone defect areas. Yet, its effects in vivo animal models require further study.

## Declaration of competing interest

The authors declared that they have no conflicts of interest to this manuscript, manuscript is approved by all authors for publication.

We declare that we do not have any commercial or associative interest that represents a conflict of interest in connection with the work submitted.

## Acknowledgments

This work was financially supported by Shanxi Basic Research Program (Free Exploration) Project (202203021211225) from Shanxi Provincial Department of Science and Technology. We gratefully acknowledge the support from Shanxi Province Key Laboratory of Oral Diseases Prevention and New Materials, Clinical Medical Research Center of Oral Diseases of Shanxi Province (Cultivation). We also thank Key Laboratory of Cellular Physiology at Shanxi Medical University, Ministry of Education, and the Department of Physiology, Shanxi Medical University.

## References

- [1] Titsinides S, Agrogiannis G, Karatzas T. Bone grafting materials in dentoalveolar reconstruction: A comprehensive review. *Jpn Dent Sci Rev* 2019;55(1): 26–32.
- [2] El Zahwy M, Taha S, Mounir R, Mounir M. Assessment of vertical ridge augmentation and marginal bone loss using autogenous onlay vs inlay grafting techniques with simultaneous implant placement in the anterior maxillary esthetic zone: A randomized clinical trial. *Clin Implant Dent Relat Res* 2019;21(6):1140–7.
- [3] Kuriakose MA, Shnayder Y, DeLacure MD. Reconstruction of segmental mandibular defects by distraction osteogenesis for mandibular reconstruction. *Head Neck* 2003;25(10):816–24.
- [4] Berner A, Reichert JC, Müller MB, Zellner J, Pfeifer C, Dienstknecht T, et al. Treatment of long bone defects and non-unions: from research to clinical practice. *Cell Tissue Res* 2012;347(3):501–19.
- [5] Kim Y, Nowzari H, Rich SK. Risk of prion disease transmission through bovine-derived bone substitutes: a systematic review. *Clin Implant Dent Relat Res* 2013;15(5):645–53.
- [6] Simpson ER, Mahendroo MS, Means GD, Kilgore MW, Hinshelwood MM, Graham-Lorence S, et al. Aromatase cytochrome P450, the enzyme responsible for estrogen biosynthesis. *Endocr Rev* 1994;15(3):342–55.
- [7] Thomas MP, Potter BV. The structural biology of oestrogen metabolism. *J Steroid Biochem Mol Biol* 2013;137:27–49.
- [8] Kumar RS, Goyal N. Estrogens as regulator of hematopoietic stem cell, immune cells and bone biology. *Life Sci* 2021;269:119091.
- [9] Lizneva D, Yuen T, Sun L, Kim SM, Atabiekov I, Munshi LB, et al. Emerging concepts in the epidemiology, pathophysiology, and clinical care of osteoporosis across the menopausal transition. *Matrix Biol* 2018;71:70–81.
- [10] Lara-Castillo N. Estrogen signaling in bone. *Appl Sci* 2021;11(10):4439.
- [11] Zhou ZH, Gu CW, Li J, Huang XY, Deng JQ, Shen LH, et al. beta-estradiol affects proliferation and apoptosis of canine bone marrow mesenchymal stem cells in vitro. *Pol J Vet Sci* 2020;23(2):235–45.
- [12] Falahati-Nini A, Riggs BL, Atkinson EJ, O'Fallon WM, Eastell R, Khosla S. Relative contributions of testosterone and estrogen in regulating bone resorption and formation in normal elderly men. *J Clin Invest* 2000;106(12): 1553–60.
- [13] Cong R, Wei G, Feng L, Ming X. Pilose antler aqueous extract promotes the proliferation and osteogenic differentiation of bone marrow mesenchymal stem cells by stimulating the BMP-2/Smad1, 5/Runx2 signaling pathway. *Chin J Nat Med* 2019;17(10):756–67.
- [14] Bhattacharjee P, Kundu B, Naskar D, Kim HW, Maiti TK, Bhattacharya D, et al. Silk scaffolds in bone tissue engineering: An overview. *Acta Biomater* 2017;63:1–17.
- [15] Shi L, Wang F, Zhu W, Xu Z, Fuchs S, Hilborn J, et al. Self-healing silk fibroin-based hydrogel for bone regeneration: dynamic metal-ligand self-assembly approach. *Adv Funct Mater* 2017:1700591.
- [16] Naskar D, Ghosh AK, Mandal M, Das P, Nandi SK, Kundu SC. Dual growth factor loaded nonmulberry silk fibroin/carbon nanofiber composite 3D scaffolds for in vitro and in vivo bone regeneration. *Biomaterials* 2017;136:67–85.
- [17] Chen HW, Lin MF. Characterization, biocompatibility, and optimization of electrospun SF/PCL/CS composite nanofibers. *Polymers (Basel)* 2020;12(7).
- [18] Wang L, Fang M, Xia Y, Hou J, Nan X, Zhao B, et al. Preparation and biological properties of silk fibroin/nano-hydroxyapatite/graphene oxide scaffolds with an oriented channel-like structure. *RSC Adv* 2020;10(17):10118–28.
- [19] Wang L, Zhang Y, Xia Y, Xu C, Meng K, Lian J, et al. Photocross-linked silk fibroin/hyaluronic acid hydrogel loaded with hDPSC for pulp regeneration. *Int J Biol Macromol* 2022;215:155–68.
- [20] Wang L, Lu R, Hou J, Nan X, Xia Y, Guo Y, et al. Application of injectable silk fibroin/graphene oxide hydrogel combined with bone marrow mesenchymal stem cells in bone tissue engineering. *Coll Surf A: Physicochem Eng Asp* 2020;604:125318.

- [21] Kaushik S, Thungon PD, Goswami P. Silk fibroin: an emerging biocompatible material for application of enzymes and whole cells in bioelectronics and bioanalytical sciences. *ACS Biomater Sci Eng* 2020;6(8):4337–55.
- [22] Ma Y, Canup BSB, Tong X, Dai F, Xiao B. Multi-responsive silk fibroin-based nanoparticles for drug delivery. *Front Chem* 2020;8:585077.
- [23] Muiznieks LD, Keeley FW. Biomechanical design of elastic protein biomaterials: a balance of protein structure and conformational disorder. *ACS Biomater Sci Eng* 2017;3(5):661–79.
- [24] Li M, Ogiso M, Minoura N. Enzymatic degradation behavior of porous silk fibroin sheets. *Biomaterials* 2003;24(2):357–65.
- [25] Wang Y, Song W, Jing S, Yu J. [Effect of estrogen deficiency on the proliferation and osteogenic differentiation potential of mandibular bone marrow stromal cells]. *Zhonghua Kou Qiang Yi Xue Za Zhi* 2014;49(10):619–24.
- [26] Hong L, Zhang G, Sultana H, Yu Y, Wei Z. The effects of 17- $\beta$  estradiol on enhancing proliferation of human bone marrow mesenchymal stromal cells in vitro. *Stem Cells Dev* 2011;20(5):925–31.
- [27] Cheng Shuli DY. Inhibitory effect of estrogen on apoptosis of bone marrow mesenchymal stem cells in mice and its mechanism. *Chin J Cell Mol Immunol* 2012;28(5):514–6.
- [28] Luo Xin, Gao Lufen, Chen Cuiping, Xie Jingyan, Jiang Xuefeng, Shen Yuan. Effects of 17 $\beta$ -estradiol on the proliferation and myogenic differentiation of bone marrow mesenchymal stem cells. *Chin J Clin Obstet Gynecol* 2010;11(05):369–73.
- [29] Chuang SC, Chen CH, Chou YS, Ho ML, Chang JK. G protein-coupled estrogen receptor mediates cell proliferation through the cAMP/PKA/CREB pathway in murine bone marrow mesenchymal stem cells. *Int J Mol Sci* 2020;21(18).
- [30] Zhu XF, Wang Y, Jin Y. Estrogen promotes osteogenic differentiation of mouse bone marrow mesenchymal stem cells in a dose-dependent manner. *Zhongguo Zuzhi Gongcheng Yanjiu* 2012;16(19):3433–7.
- [31] Hong L, Sultana H, Paulius K, Zhang G. Steroid regulation of proliferation and osteogenic differentiation of bone marrow stromal cells: a gender difference. *J Steroid Biochem Mol Biol* 2009;114(3–5):180–5.
- [32] Peng H, Guo Q, Xiao Y, Su T, Jiang TJ, Guo LJ, et al. ASPH regulates osteogenic differentiation and cellular senescence of BMSCs. *Front Cell Dev Biol* 2020;8:872.